Intruder negative-parity states of neutron-rich ^{33}Si

Z. M. Wang,[1,*] R. Chapman,[1] X. Liang,[1] F. Haas,[2] M. Bouhelal,[2] F. Azaiez,[3] B. R. Behera,[4] M. Burns,[1] E. Caurier,[2] L. Corradi,[4] D. Curien,[2] A. N. Deacon,[5] Zs. Dombrádi,[6] E. Farnea,[7] E. Fioretto,[4] A. Gadea,[4] A. Hodsdon,[1] F. Ibrahim,[3] A. Jungclaus,[8] K. Keyes,[1] V. Kumar,[1] A. Latina,[4] N. Mărginean,[4,9] G. Montagnoli,[7] D. R. Napoli,[4] F. Nowacki,[2] J. Ollier,[1,10] D. O'Donnell,[1,10] A. Papenberg,[1] G. Pollarolo,[11] M.-D. Salsac,[12] F. Scarlassara,[7] J. F. Smith,[1] K. M. Spohr,[1] M. Stanoiu,[9] A. M. Stefanini,[4] S. Szilner,[4,13] M. Trotta,[4] and D. Verney[3]

[1]*School of Engineering, University of the West of Scotland, Paisley, PA1 2BE, United Kingdom and the Scottish Universities Physics Alliance (SUPA)*

[2]*IPHC, CNRS-IN2P3, and Université de Strasbourg, F-67037 Strasbourg Cedex 2, France*

[3]*IPN, CNRS-IN2P3, and Université Paris-Sud, F-91406 Orsay Cedex, France*

[4]*INFN, Laboratori Nazionali di Legnaro, I-35020 Legnaro, Padova, Italy*

[5]*Schuster Laboratory, University of Manchester, Manchester, M13 9PL, United Kingdom*

[6]*ATOMKI, P. O. Box 51, H-4001 Debrecen, Hungary*

[7]*INFN–Sezione di Padova and Dipartimento di Fisica, Università di Padova, I35131 Padova, Italy*

[8]*Instituto de Estructura de la Materia, CSIC, E-28006 Madrid, Spain*

[9]*Horia Hulubei National Institute of Physics and Nuclear Engineering, Strasse Atomistilor 407, P. O. Box MG-6, Bucharest, Romania*

[10]*STFC Daresbury Laboratory, Warrington, WA4 4AD, United Kingdom*

[11]*Dipartimento di Fisica Teorica, Università di Torino, and INFN–Sezione di Torino, Via P. Giuria 1, I-10125 Torino, Italy*

[12]*CEA-Saclay, Service de Physique Nucléaire, 91191 Gif-sur-Yvette, France*

[13]*Ruđer Bošković Institute, Zagreb, Croatia*

(Received 15 April 2010; published 1 June 2010)

Yrast states in the neutron-rich $^{33}_{14}Si_{19}$ nucleus have been studied using binary grazing reactions produced by the interaction of a 215-MeV beam of ^{36}S ions with a thin ^{208}Pb target. An experimental setup that combines the large-acceptance magnetic spectrometer PRISMA and the high-efficiency γ-ray detection array CLARA was used in the experiment. Four new γ-ray photopeaks at energies of 971, 1724, 1772, and 2655 keV were observed and assigned to the ^{33}Si level scheme. The experimental level scheme is compared with the results of $1\hbar\omega$ *p-sd-pf* large-scale shell-model calculations using the recently developed PSDPFB effective interaction; good agreement is obtained. The structure of the populated states of ^{33}Si is discussed within the context of an odd neutron coupled to states of the ^{32}Si core.

DOI: 10.1103/PhysRevC.81.064301 PACS number(s): 23.20.Lv, 25.70.Lm, 27.30.+t

I. INTRODUCTION

The region of neutron-rich nuclei around $N = 20$ continues to be the subject of active research, both experimental and theoretical; this is the region in which the breaking of a shell closure far from stability was first observed in $^{32}_{12}Mg_{20}$ [1–3], and interpreted within a shell-model context as arising from a two particle–two hole intruder configuration [4,5]. $^{34}_{14}Si_{20}$ lies outside the island of inversion and, although only two protons removed from the highly deformed $^{32}_{12}Mg_{20}$ nucleus, is a spherical $N = 20$ closed-shell nucleus in its ground state. Further, although there is some uncertainty in the energy gap between the proton $1d_{5/2}$ orbital (fully occupied in a simple shell-model picture of the ^{34}Si ground state) and the $2s_{1/2}$ orbital (empty in the ^{34}Si ground state) as a consequence of an incomplete knowledge of the fragmentation of the proton $1d_{5/2}$ single-particle strength, the separation is known to be large, giving the nucleus the characteristics of a doubly magic nucleus. In the work of Cottle [6], the splitting is given as about 7 MeV for ^{34}Si. In its ground state, ^{33}Si has a neutron hole in the $1d_{3/2}$ orbit; neutron one particle–two hole configurations will therefore play a dominant role in the structure of negative-parity states. With a neutron promoted to the $1f_{7/2}$ orbit, the monopole tensor force [7] will influence the binding of the proton single-particle orbits below the $Z = 20$ shell closure. The attractive tensor force will lead to a stronger binding of the $1d_{3/2}$ ($j_<$) state, leading to a smaller energy gap between the $1d_{3/2}$ and $2s_{1/2}$ proton orbitals. The evolution of the $E(1/2^+)$-$E(3/2^+)$ energy spacing for odd-mass K, Cl, and P isotopes with neutron numbers in the range from 20 to 28 has been reported by Gade *et al.* [8].

^{33}Si has previously been studied using deep inelastic collision processes with a thick target [9–11], in multinucleon transfer reactions [12,13], in one-neutron knockout reactions [14], and in β decay [15]. The ground-state J^π value has been assigned as $3/2^+$, on the basis of one-neutron transfer studies [14] and shell-model predictions. The assignment is in agreement with the systematics of $N = 19$ isotones in this neutron-rich mass region [16].

Knowledge of the nuclear structure of ^{33}Si is somewhat limited, and here we attempt to address this in an experiment that utilized an experimental setup involving the coupling of the large-acceptance magnetic spectrometer PRISMA [17] and the high-granularity and high-efficiency γ-ray Ge detector array CLARA [18]. The ability to perform Doppler correction,

*zhimin.wang@uws.ac.uk

on an event-by-event basis, of the energies of γ rays emitted by nuclei moving with velocities of the order of $v/c \sim 0.1$, together with good reaction-channel selection, enables high-quality singles γ-ray spectra to be produced. In this paper, the level structure is compared with the results of large-scale $1\hbar\omega$ shell-model calculations based on a ^{4}He core and which use the recently developed PSDPFB effective interaction [19–21].

The present work forms one of several studies of neutron-rich nuclei in the *sdpf* shell that are based on results from the same experiment. To date, we have reported on the structure of ^{36}Si [22], ^{37}P [23], ^{40}S [24], and ^{38}Cl [25]. Earlier related studies of neutron-rich nuclei populated in deep inelastic collisions with thick targets have focused on the structure of ^{34}P [26], ^{36}S [27], and ^{41}Cl [28,29]. These published works are mainly concerned with the role of negative-parity intruder orbitals in the structure of neutron-rich nuclei on the periphery of the island of inversion.

II. EXPERIMENT

The neutron-rich nucleus ^{33}Si was populated in binary grazing reactions produced by a 215-MeV beam of $^{36}S^{9+}$ ions, delivered by the Tandem-ALPI accelerator complex at the INFN Legnaro National Laboratory, Italy, incident on a thin ^{208}Pb target. The target, isotopically enriched to 99.7% in ^{208}Pb, was of thickness 300 μg cm^{-2} on a 20 μg cm^{-2} carbon backing.

Projectile-like fragments produced during the reaction were analyzed with PRISMA, a large acceptance-angle magnetic spectrometer ($\pm 5.5^\circ$ in the dispersion plane and $\pm 10.5^\circ$ perpendicular to the dispersion plane, ~80 msr solid angle), placed at 56° to the beam axis, and covering a range of angles including the grazing angle of the reaction (~58°). The PRISMA spectrometer consists of a quadrupole singlet and a dipole magnet separated by 60 cm. The (x,y) coordinates and time information of each ion entering the spectrometer are measured using a position-sensitive microchannel plate (MCP) detector [30] placed at 25 cm from the target. Following the passage of each ion through the magnetic elements, the coordinates and time information are measured again at the focal plane of the spectrometer using a ten-element 100 cm long multiwire parallel-plate avalanche counter (MWPPAC) [31]. The position resolution of the MCP and MWPPAC is 1 mm in the horizontal (dispersive) direction and the time resolution of the MCP and MWPPAC combination is about ~300 ps. Finally, the ions are stopped in a 10 × 4 element ionization chamber used for energy loss, ΔE, and total energy, E, measurements [30,31]. For each ion that reaches the focal plane of PRISMA, the above measurements enable us to determine the time of flight, the mass number A, the atomic number Z, and the ion charge state, thereby allowing an unambiguous identification of each detected projectile-like nucleus. Reconstruction of the trajectory of each ion through the spectrometer together with the time-of-flight measurement was used to establish the velocity vector of each detected ion on an event-by-event basis.

Gamma rays from the deexcitation of the binary reaction products were detected using CLARA, an array of 25 escape-suppressed Ge clover detectors (22 Ge clover detectors were used during the present work). Gamma rays were detected in time coincidence with projectile-like fragments identified at the focal plane of the PRISMA spectrometer, leading to an unambiguous assignment of each γ-ray photopeak to a nucleus of selected A and Z. CLARA was positioned in the hemisphere opposite to the PRISMA spectrometer and covering the azimuthal angles from 98° to 180° with respect to the entrance aperture of PRISMA. For 1.3-MeV γ rays from a ^{60}Co source, the CLARA total photopeak efficiency is ~2.8%, and the peak-to-total ratio is ~45%. Doppler correction of γ-ray energies was performed on an event-by-event basis. The energy resolution of γ-ray photopeaks following Doppler correction was typically ~0.6%. Experimental data were accumulated during a six-day run with an average beam current of 60 *e* nA.

III. RESULTS AND DISCUSSION

In the present experiment, projectile-like nuclear species from magnesium ($Z = 12$) to calcium ($Z = 20$) were identified at the focal plane of PRISMA. In this paper, we focus on the nuclear structure of the neutron-rich silicon isotope ^{33}Si. The mass spectrum of silicon ($Z = 14$) isotopes ranging from ^{30}Si to ^{36}Si is shown in Fig. 1. The mass resolution was measured as ~1/140. With the A and Z identification available from the PRISMA spectrometer, it is possible to select individual projectile-like nuclear species produced in the reaction.

The Doppler-corrected one-dimensional γ-ray spectrum corresponding to a gate set on ^{33}Si in the mass spectrum of Fig. 1 is shown in Fig. 2. In total, approximately 7×10^4 ^{33}Si ions were detected in coincidence with at least one γ ray. Characteristic lead x rays are marked as such in Fig. 2, while very broad photopeaks from unobserved associated target-like reaction partners (mainly ^{208,209,210}Po), inappropriately Doppler corrected, are marked as *C* in Fig. 2. The measured γ-ray energies with associated uncertainties, relative intensities, and proposed placement in the level scheme of ^{33}Si are presented in Table I. In the present work, γ-ray

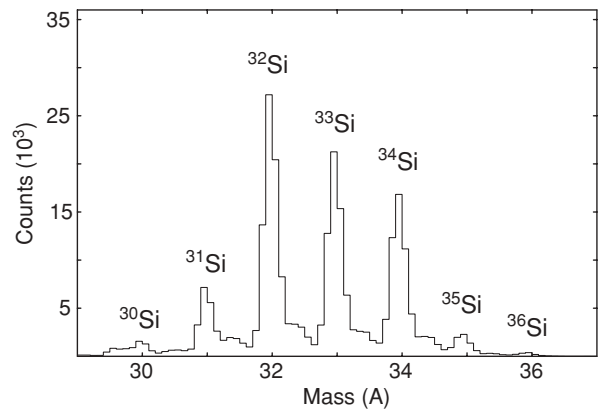

FIG. 1. A mass spectrum for silicon isotopes populated in the present work.

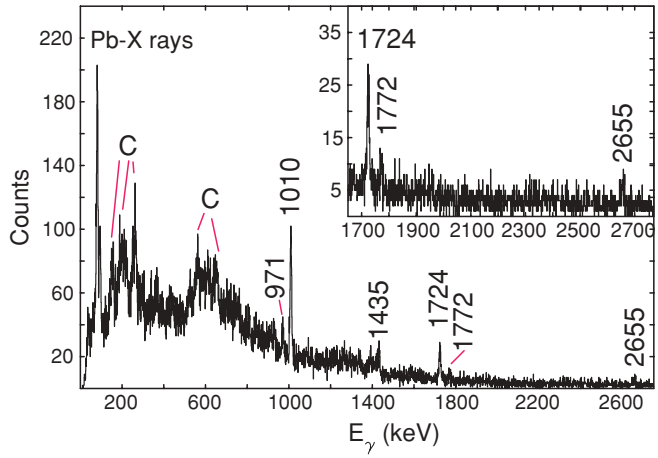

FIG. 2. (Color online) A γ-ray spectrum corresponding to the deexcitation of ^{33}Si nuclei. See text for details.

coincidence measurements are not possible because of the low statistics.

The previously reported γ-ray transitions in ^{33}Si are those at energies of 1010.2, 1434.9, and 4341 keV ([16] and references therein). Gamma-ray photopeaks at energies of 1010 and 1435 keV are clearly seen in the spectrum of Fig. 2. The 4341-keV γ-ray transition is not observed in the present study; its energy lies outside the current range of measured energies. In addition, there are four previously unobserved photopeaks at energies of 971, 1724, 1772, and 2655 keV.

The 1010- and 1435-keV γ-ray transitions were observed in earlier deep inelastic studies using thick targets [9–11] (see Fig. 3). The 1435-keV stretched $M2$ transition connects the isomeric $7/2^-$ state to the $3/2^+$ ground state. The stretched $M2$ assignment was based on an in-plane/out-of-plane γ-ray asymmetry analysis and on the measured 10.2(3) ns half-life [32]. The 4341-keV γ-ray transition was observed in β-decay studies [15]. We have revisited two sets of data obtained in deep inelastic studies that involved the bombardment of a thick target of ^{160}Gd by 234-MeV ^{37}Cl ions [28,33] and the bombardment of a thick target of ^{176}Yb by 230-MeV ^{36}S ions [11]. Of the photopeaks listed in Table I, only the 1010- and 1435-keV γ-ray transitions could be identified. This strongly suggests that the yrast states above the 1435-keV isomer have lifetimes of the order of 1 ps or shorter. In in-beam γ-ray spectroscopy studies of binary reaction fragments from deep inelastic processes using thick targets, γ rays depopulating states with lifetimes less than about 1 ps are generally not observed experimentally since the nuclear lifetime is comparable to the slowing-down time of the nucleus in the target material; the γ-ray photopeaks are consequently Doppler broadened and cannot be observed. The present experiment does not suffer from this limitation, but there is a loss of observed γ-ray intensity for decays from states with lifetimes in excess of a few nanoseconds. The long half-life [10.2(3) ns] of the yrast $(7/2^-)$ state combined with the large velocity of projectile-like fragments ($\upsilon/c \sim 0.1$), results in only about 30% of 1435-keV γ rays being observed in the present experiment. Further, deexcitation of the 1435-keV state occurs along the trajectory of the ^{33}Si nucleus as it moves from the target to the entrance of the PRISMA spectrometer. This results in a broadened line shape for the 1435-keV peak in the γ-ray spectrum.

TABLE I. Measured γ-ray energies and relative intensities of transitions in ^{33}Si observed in the present experiment.

E_γ (keV)	I_γ/I_{1010} %	$E_i \rightarrow E_f$ (keV)
971(1)	22(3)	1981 → 1010
1010(1)	100(5)	1010 → 0
1435(2)	86(7)	1435 → 0
1724(2)	49(4)	3159 → 1435
1772(2)	14(2)	4931 → 3159
2655(2)	24(3)	4090 → 1435

A series of levels at energies of 0, 1470, 2000, 3190, 4130, and 5480 keV were established by Fifield *et al.* in the ^{34}S(^{13}C,^{14}O) transfer reaction [13]. The 1470- and 2000-keV states were assigned J^π values of $(7/2^-)$ and $(3/2^-)$, respectively, based on model-dependent arguments. In the earlier work of Fifield *et al.,* [12] states of ^{33}Si were populated in the ^{36}S(^{11}B,^{14}N) multinucleon transfer reaction. The populated states at excitation energies of 0, 1060, and 4320 keV were assigned J^π values of $(3/2^+)$, $(1/2^+)$, and $(5/2^+)$, respectively, again based on model-dependent arguments. More recently, single-neutron knockout to ^{33}Si has been studied by Enders *et al.* [14] using a 73 A MeV beam of ^{34}Si. The quantum numbers of the removed neutron and spectroscopic factors were determined. States of ^{33}Si at 0, 1.010, and 4.290 MeV were populated and were assigned J^π values of $3/2^+$, $1/2^+$, and $5/2^+$, respectively. The measured spectroscopic factors are consistent with full occupancy of the neutron $1d_{3/2}$ and $2s_{1/2}$ orbitals in the ground state of ^{34}Si.

In placing the previously unobserved γ-ray transitions of energy 971, 1724, and 2655 keV in the level scheme of ^{33}Si, we have been guided by the work of Fifield *et al.* [12,13], by γ-ray intensity considerations, and by the observation that binary grazing reactions preferentially populate yrast and near-yrast states [9,26,27,34].

A comparison of the ^{33}Si level energies of 1010 and 1435 keV with those measured by Fifield *et al.* [12,13] at 1060 and 1470 keV reveals a difference of $\sim$ 40 keV. The difference, it is suggested here, comes from a systematic experimental uncertainty in the energy measurement for the transfer reaction studies of Fifield *et al.* We tentatively assign the 971-keV γ ray, observed in the present work, to the transition from the 1981-keV $J^\pi = (3/2^-)$ state, previously identified by Fifield *et al.* at 2000 keV, to the 1010-keV state. The 1724-keV γ ray, we suggest here, is associated with the transition from a 3159-keV level, previously identified by Fifield *et al.* at 3190 keV, to the yrast 1435-keV state with $J^\pi = 7/2^-$. We also tentatively assign the 2655-keV γ-ray to the transition from the 4090-keV state, identified by Fifield *et al.* at 4130 keV, to the 1435-keV state. The 1772-keV γ ray is tentatively assigned to the transition between the hitherto unobserved 4931-keV state to the 3159-keV state; this assignment is based purely on intensity considerations and should be regarded as speculative. A comparison of the present proposed level energies with the results of Fifield *et al.* [12,13] shows

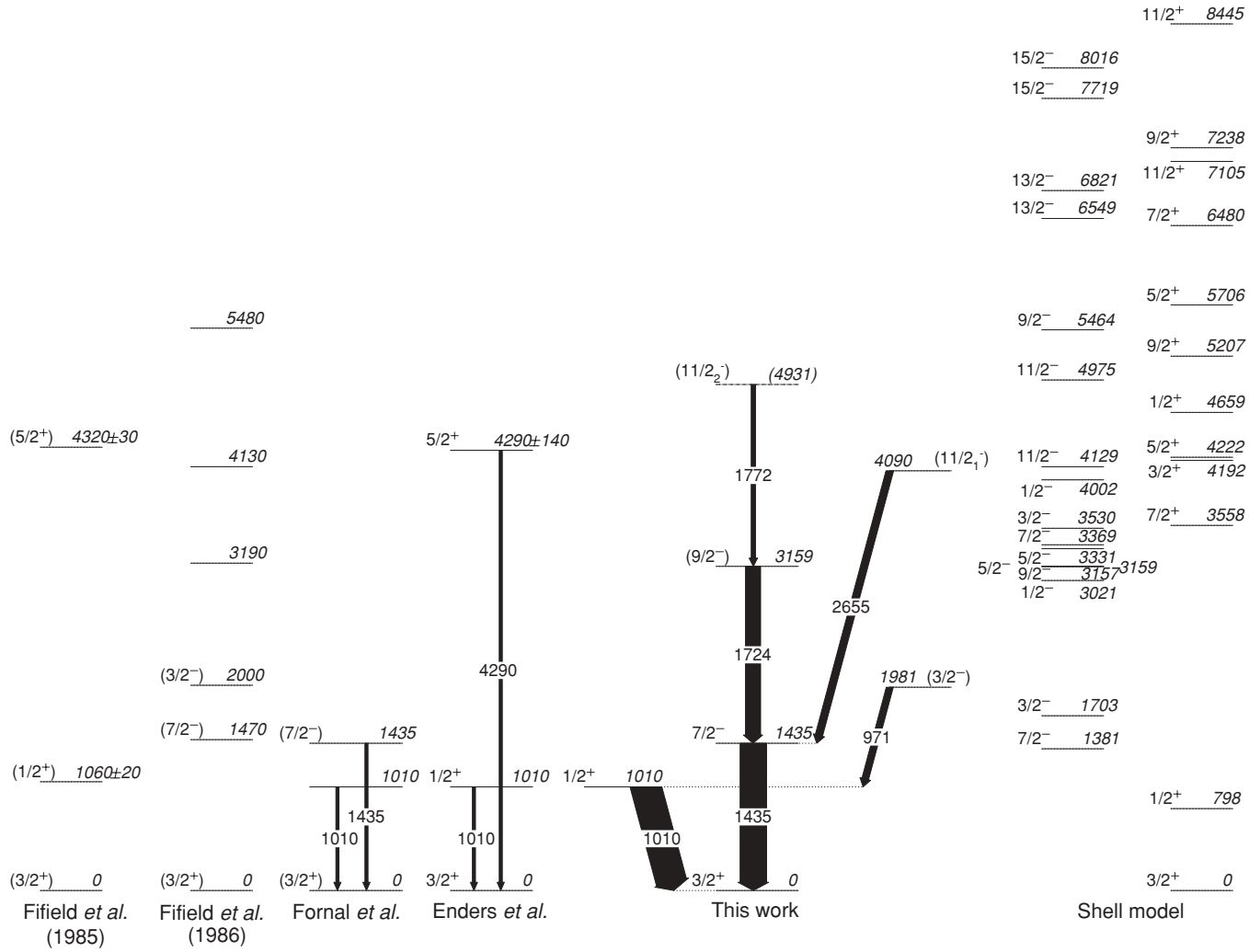

FIG. 3. A comparison of previous experimental results from multinucleon transfer reactions [12,13], deep inelastic processes [9–11], and neutron knockout reactions [14] with the present proposed level scheme of ^{33}Si. The width of the arrows is proportional to the relative transition intensities. The results of large-scale $1\hbar\omega$ *p-sd-pf* shell-model calculations are also shown. Only the first two states of each J^π value are presented. J^π assignments for the states of ^{33}Si observed in the present work are based on experimental and model-dependent arguments. See text for details.

a continuing systematic trend; the present level energies are smaller than those of Fifield *et al.* by around 20–40 keV; see Fig. 3. It is noted here that, in the earlier reported study of ^{37}P [23], populated in the experiment discussed here, five of the seven observed γ-ray transitions were accommodated within the corrected level scheme of Orr [35], which was based on a study of the ^{36}S(^{18}O,^{17}F)^{37}P reaction. Based on the observation that yrast states are generally the most strongly populated in multinucleon grazing reactions, we suggest here that the state at 3159 keV has J values of $(9/2, 11/2)$, the state at 4090 keV has J values of $(9/2, 11/2)$, and the state at 4931 keV has J values of $(11/2, 13/2)$. The Weisskopf estimate for the lifetime of a 1724-keV $M2$ transition is about 200 ps. $M2$ transitions are generally inhibited compared to the Weisskopf estimate by a factor of at least 10 [36]; on the basis that this transition should have been observed in the thick-target data discussed earlier, we can exclude a J^π value of $11/2^+$ for the 3159-keV state. In Fig. 3, the J^π values of the states at 3159, 4090, and 4931 keV are based on experimental and on model-dependent arguments, which follow. In the level scheme from the present work, the J^π values for the ground and first three excited states are taken from the earlier studies that were discussed above.

To investigate the single-particle structure of the states of ^{33}Si, we have performed large-scale $1\hbar\omega$ shell-model calculations using the NATHAN code [37,38] with a new PSDPFB effective interaction [19–21] that is based on a ^{4}He core. In the interaction, one nucleon is allowed to jump between the p and sd or between the sd and pf shells. The results of the calculations performed here show that, for the ^{33}Si states, the protons are confined within the sd shell and that the negative-parity states result from the excitation of one neutron across the $N = 20$ gap into the pf shell. A comparison of the experimental level scheme with the results of the $1\hbar\omega$ *p-sd-pf*

TABLE II. The main components of the wave functions of the levels of ^{33}Si from the large-scale $1\hbar\omega$ *p-sd-pf* shell-model calculations using the PSDPFB effective interaction. See text for details.

J^π	E_x (keV)	Main components of wave function	Percentage ($\geqslant$10%)
$1/2^+$	798	$\pi(1d_{5/2})^6 \bigotimes \upsilon(2s_{1/2})^1(1d_{3/2})^4$	59
		$\pi(1d_{5/2})^5(2s_{1/2})^1 \bigotimes \upsilon(1d_{3/2})^3$	20
$3/2^+$	0	$\pi(1d_{5/2})^6 \bigotimes \upsilon(1d_{3/2})^3$	71
$5/2^+$	4222	$\pi(1d_{5/2})^6 \bigotimes \upsilon(1d_{5/2})^5(2s_{1/2})^2(1d_{3/2})^4$	26
		$\pi(1d_{5/2})^5(2s_{1/2})^1 \bigotimes \upsilon(2s_{1/2})^1(1d_{3/2})^4$	14
		$\pi(1d_{5/2})^5(2_{1/2})^1 \bigotimes \upsilon(1d_{3/2})^3$	22
$7/2^+$	3558	$\pi(1d_{5/2})^5(2s_{1/2})^1 \bigotimes \upsilon(1d_{3/2})^3$	73
$9/2^+$	5207	$\pi(1d_{5/2})^5(2s_{1/2})^0(1d_{3/2})^1 \bigotimes \upsilon(1d_{3/2})^3$	13
		$\pi(1d_{5/2})^5(2s_{1/2})^1 \bigotimes \upsilon(1d_{3/2})^3$	69
$11/2^+$	7105	$\pi(1d_{5/2})^5(2s_{1/2})^0(1d_{3/2})^1 \bigotimes \upsilon(1d_{3/2})^3$	81
$13/2^+$	11089	$\pi(1d_{5/2})^4(2s_{1/2})^1(1d_{3/2})^1 \bigotimes \upsilon(1d_{3/2})^3$	87
$15/2^+$	12774	$\pi(1d_{5/2})^4(2s_{1/2})^0(1d_{3/2})^2 \bigotimes \upsilon(1d_{3/2})^3$	13
		$\pi(1d_{5/2})^4(2s_{1/2})^1(1d_{3/2})^1 \bigotimes \upsilon(1d_{3/2})^3$	75
$1/2^-$	3021	$\pi(1d_{5/2})^6 \bigotimes \upsilon(1d_{3/2})^4(2p_{1/2})^1$	12
		$\pi(1d_{5/2})^6 \bigotimes \upsilon(1d_{3/2})^2(2p_{1/2})^1$	19
$3/2^-$	1703	$\pi(1d_{5/2})^4(2s_{1/2})^2 \bigotimes \upsilon(1d_{3/2})^2(2p_{3/2})^1$	10
		$\pi(1d_{5/2})^6 \bigotimes \upsilon(1d_{3/2})^2(2p_{3/2})^1$	34
$5/2^-$	3159	$\pi(1d_{5/2})^6 \bigotimes \upsilon(1d_{3/2})^2(1f_{5/2})^1$	11
$7/2^-$	1381	$\pi(1d_{5/2})^6 \bigotimes \upsilon(1d_{3/2})^2(1f_{7/2})^1$	29
$9/2^-$	3157	$\pi(1d_{5/2})^5(2s_{1/2})^1 \bigotimes \upsilon(1d_{3/2})^2(1f_{7/2})^1$	19
		$\pi(1d_{5/2})^6 \bigotimes \upsilon(1d_{3/2})^2(1f_{7/2})^1$	11
$11/2_1^-$	4129	$\pi(1d_{5/2})^5(2s_{1/2})^1 \bigotimes \upsilon(1d_{3/2})^2(1f_{7/2})^1$	12
		$\pi(1d_{5/2})^6 \bigotimes \upsilon(1d_{3/2})^2(1f_{7/2})^1$	27
$11/2_2^-$	4974	$\pi(1d_{5/2})^6 \bigotimes \upsilon(2s_{1/2})^1(1d_{3/2})^3(1f_{7/2})^1$	15
		$\pi(1d_{5/2})^5(2s_{1/2})^1 \bigotimes \upsilon(1d_{3/2})^2(1f_{7/2})^1$	18
		$\pi(1d_{5/2})^6 \bigotimes \upsilon(1d_{3/2})^2(1f_{7/2})^1$	16
$13/2^-$	6549	$\pi(1d_{5/2})^6 \bigotimes \upsilon(1d_{5/2})^5(2s_{1/2})^2(1d_{3/2})^3(1f_{7/2})^1$	13
		$\pi(1d_{5/2})^5(2s_{1/2})^1 \bigotimes \upsilon(1d_{3/2})^2(1f_{7/2})^1$	17
$15/2^-$	7719	$\pi(1d_{5/2})^6 \bigotimes \upsilon(1d_{5/2})^5(2s_{1/2})^2(1d_{3/2})^3(1f_{7/2})^1$	10
		$\pi(1d_{5/2})^5(2s_{1/2})^1 \bigotimes \upsilon(1d_{3/2})^2(1f_{7/2})^1$	19

shell-model calculation is presented in Fig. 3. We can see that the new PSDPFB effective interaction is able to reproduce the experimental level energies well. There is reasonably strong evidence for shell-model states corresponding to the excited states observed at 1010, 1435, 1981, 3159, 4090, and 4931 keV. In the shell-model calculations, the yrast excited states have negative parity. On this basis, the observed states above 1010 keV have negative parity, with J^π values in the range from $(3/2^-)$ to $(11/2^-)$ (see Fig. 3). Here it is noted, as a word of caution, that the suggested negative-parity assignments to the states of ^{33}Si observed here are speculative and not based on experimental observation.

Table II presents the main components of the shell-model wave functions of the states of ^{33}Si. For completeness, the wave functions of positive-parity states up to J^π values of $15/2^+$ are given. The positive-parity yrast states have rather pure configurations, based on proton occupation of the $1d_{5/2}$, $2s_{1/2}$, and $1d_{3/2}$ shell-model orbitals with neutron occupation of the $1d_{3/2}$ orbital. In contrast, the wave functions of the $1p$-$2h$ negative-parity states are more mixed, and correspond mainly to two holes in the $1d_{3/2}$ neutron orbital with a neutron occupying the *pf* shell. Thus, while the $J^\pi = 15/2^+$ state has one dominant component in its wave function, the wave function of the $J^\pi = 15/2^-$ state has no component larger than 20% (see Table II). The shell-model half-life of the 1435-keV state is 6.3 ns, which compares favorably with the measured value of 10.2(3) ns; the multipolarity of the transition is dominated by $M2$, again in agreement with observation [32]. The relatively long shell-model lifetime of the 1010-keV state of 35 ps is consistent with the observation

TABLE III. The main components of the wave functions of the negative-parity states of ^{33}Si from large-scale $1\hbar\omega$ *p-sd-pf* shell-model calculations using the PSDPFB effective interaction. The wave functions are expressed in terms of an odd neutron coupled to the states of ^{32}Si.

J^π	E_x (keV)	Main components of wave function	Percentage ($\geqslant$10%)
$3/2^-$	1703	$\upsilon(2p_{3/2})^1 \otimes 0^+$	64
$7/2^-$	1381	$\upsilon(1f_{7/2})^1 \otimes 0^+$	57
		$\upsilon(1f_{7/2})^1 \otimes 2^+$	21
$9/2^-$	3157	$\upsilon(1f_{7/2})^1 \otimes 2^+$	75
$11/2^-_1$	4129	$\upsilon(1f_{7/2})^1 \otimes 2^+$	70
$11/2^-_2$	4974	$\upsilon(1f_{7/2})^1 \otimes 2^+$	59

of its decay in thick-target experiments in which multinucleon transfer processes were used to populate the nucleus [9–11]; the lifetime is much longer than the slowing-down time ($\sim$1 ps) of recoiling ^{33}Si nuclei in the target material. The 1010-keV transition has also been observed in an intermediate energy Coulomb excitation experiment [39]; the experimental $B(E2; 3/2^+ \rightarrow 1/2^+)$ value of 16.5 $\pm$ 3.2 e^2 fm^4 is very well reproduced in the present shell-model calculations, which give a $B(E2)$ value of 17.1 e^2 fm^4. The 971-keV transition depopulates the 1981-keV state which has a predicted lifetime of 17 ps. The transition should consequently be observed in thick-target measurements; that it was not observed can be explained by the weak population of the non-yrast state. The shell-model lifetimes of the 3159-, 4090-, and 4931-keV states are 0.16, 0.25, and 0.54 ps, respectively. The short lifetimes are consistent with the non-observations of the decay γ rays in the earlier thick-target measurements. Table III presents the main components of the wave functions for the yrast and near-yrast negative-parity states of ^{33}Si corresponding to the new PSDPFB effective interaction. Here, the wave functions are expressed in terms of the coupling of an odd neutron to the $J^\pi = 0^+_{\text{g.s.}}$ and 2^+_1 states of the ^{32}Si core. It can be seen that the $J^\pi = 9/2^-, 11/2^-_1$, and $11/2^-_2$ states have large components in their wave functions corresponding to the coupling of a $1f_{7/2}$ neutron to the $J^\pi = 2^+_1$ excitation of ^{32}Si. This is not entirely surprising since the negative-parity intruder states of ^{33}Si have $1p$-$2h$ neutron configurations, that is, a single neutron in the pf shell coupled to a ^{32}Si core. The transitions from the $9/2^-$ and $11/2^-_1$ states to the $7/2^-$ state at 1435 keV proceed mainly through deexcitation of the 2^+_1 state of ^{32}Si to the ground state, with the $1f_{7/2}$ neutron acting as a spectator.

IV. SUMMARY

In the present work, the neutron-rich ^{33}Si isotope was populated using binary grazing reactions. The PRISMA magnetic spectrometer in conjunction with the CLARA Ge array at the INFN Legnaro National Laboratory was used to identify the ^{33}Si isotope and its associated deexcitation γ rays. Relative intensity measurements of the observed γ rays together with the results of earlier multinucleon transfer experiments [12,13] were used to construct a level scheme which includes, in particular, four new γ-ray transitions at energies of 971, 1724, 1772, and 2655 keV. We propose that these transitions correspond to the deexcitation of excited states at 1981, 3159, 4931, and 4090 keV, with corresponding J^π values of $(3/2^-)$, $(9/2^-)$, $(11/2^-_2)$, and $(11/2^-_1)$, respectively. The results of shell-model calculations with a new PSDPFB effective interaction [19–21], which is based on a ^{4}He core, agree well with the experimental energy spectrum of ^{33}Si and indicate that the higher-spin negative-parity states of ^{33}Si can be described in terms of the coupling of an odd $1f_{7/2}$ neutron to the $J^\pi = 2^+_1$ state of the ^{32}Si core.

ACKNOWLEDGMENTS

This work was supported in part by the EPSRC (UK) and by the European Union under Contract No. RII3-CT-2004-506065. Five of us (D.O., M.B., A.H., K.K., and A.P.) acknowledge financial support from the EPSRC. Z.M.W acknowledges support from ORSAS and from the University of the West of Scotland. A.J. acknowledges financial support from the Spanish Ministerio de Ciencia e Innovación under Contract Nos. FPA2007-66069 and FPA2009-13377-C02-02. Zs.D. acknowledges the financial support from OTKA Project No. K68801. The contribution of the accelerator and target-fabrication staff at the INFN Legnaro National Laboratory is gratefully acknowledged.

[1] T. Motobayashi *et al.*, Phys. Lett. B **346**, 9 (1995).
[2] B. V. Pritychenko *et al.*, Phys. Lett. B **461**, 322 (1999).
[3] V. Chiste *et al.*, Phys. Lett. B **514**, 233 (2001).
[4] A. Poves and J. Retamosa, Phys. Lett. B **184**, 311 (1987).
[5] B. J. Cole, A. Watt, and R. R. Whitehead, J. Phys. A **7**, 1374 (1974).
[6] P. D. Cottle, Phys. Rev. C **76**, 027301 (2007).
[7] T. Otsuka, T. Suzuki, R. Fujimoto, H. Grawe, and Y. Akaishi, Phys. Rev. Lett. **95**, 232502 (2005).
[8] A. Gade *et al.*, Phys. Rev. C **74**, 034322 (2006).
[9] B. Fornal *et al.*, Phys. Rev. C **49**, 2413 (1994).
[10] X. Liang, Ph.D. thesis, University of Paisley (2001).
[11] J. Ollier, Ph.D. thesis, University of Paisley (2004).
[12] L. K. Fifield, C. L. Woods, R. A. Bark, P. V. Drumm, and M. A. C. Hotchkis, Nucl. Phys. A **440**, 531 (1985).
[13] L. K. Fifield, C. L. Woods, W. N. Catford, R. A. Bark, P. V. Drumm, and K. T. Keoghan, Nucl. Phys. A **453**, 497 (1986).
[14] J. Enders *et al.*, Phys. Rev. C **65**, 034318 (2002).
[15] A. C. Morton *et al.*, Phys. Lett. B **544**, 274 (2002).
[16] Evaluated nuclear structure data file (ensdf) [http://www.nndc.bnl.gov/ensdf].
[17] A. M. Stefanini *et al.*, Nucl. Phys. A **701**, 217c (2002).
[18] A. Gadea *et al.* (EUROBALL Collaboration and PRISMA-2 Collaboration), Eur. Phys. J. A **20**, 193 (2004).
[19] M. Bouhelal, F. Haas, E. Caurier, F. Nowacki, and A. Bouldjedri, Acta Phys. Pol. B **40**, 639 (2009).

[20] M. Bouhelal, F. Haas, E. Caurier, F. Nowacki, and A. Bouldjedri, Eur. Phys. J. A **42**, 529 (2009).
[21] M. Bouhelal, Ph.D. thesis, University of Batna, Batna, Algeria and University of Strasbourg (2010).
[22] X. Liang *et al.*, Phys. Rev. C **74**, 014311 (2006).
[23] A. Hodsdon *et al.*, Phys. Rev. C **75**, 034313 (2007).
[24] Z. M. Wang *et al.*, Phys. Rev. C **81**, 054305 (2010).
[25] D. O'Donnell *et al.*, Phys. Rev. C **81**, 024318 (2010).
[26] J. Ollier *et al.*, Phys. Rev. C **71**, 034316 (2005).
[27] X. Liang *et al.*, Phys. Rev. C **66**, 014302 (2002).
[28] X. Liang *et al.*, Phys. Rev. C **66**, 037301 (2002).
[29] J. Ollier *et al.*, Eur. Phys. J. A **20**, 111 (2004).
[30] G. Montagnoli *et al.*, Nucl. Instrum. Methods Phys. Res. A **547**, 455 (2005).
[31] S. Beghini *et al.*, Nucl. Instrum. Methods Phys. Res. A **551**, 364 (2005).
[32] M. Asai, T. Ishii, A. Makishima, M. Ogawa, and M. Matsuda, Japan Atomic Energy Res. Inst. Tandem VDG Ann. Rept., 2001, p. 23 (2002); JAERI-Review 2002-029 (2002) (unpublished).
[33] X. Liang *et al.*, Eur. Phys. J. A **10**, 41 (2001).
[34] H. Takai *et al.*, Phys. Rev. C **38**, 1247 (1988).
[35] N. A. Orr, Ph.D. thesis, Australian National University (1989).
[36] D. Kurath and R. D. Lawson, Phys. Rev. **161**, 915 (1967).
[37] E. Caurier and F. Nowacki, Acta Phys. Pol. B **30**, 705 (1999).
[38] E. Caurier, G. Martinez-Pinedo, F. Nowacki, A. Poves, and A. P. Zuker, Rev. Mod. Phys. **77**, 427 (2005), and references therein.
[39] B. V. Pritychenko, T. Glasmacher, B. A. Brown, P. D. Cottle, R. W. Ibbotson, K. W. Kemper, and H. Scheit, Phys. Rev. C **62**, 051601(r) (2000).